Measured deviations from the saddle potential description of clean quantum point contacts

2008 J. Phys.: Condens. Matter 20 164207

(http://iopscience.iop.org/0953-8984/20/16/164207)

J. Phys.: Condens. Matter **20** (2008) 164207 (5pp) doi:10.1088/0953-8984/20/16/164207

Measured deviations from the saddle potential description of clean quantum point contacts

Poul Erik Lindelof and Martin Aagesen

Niels Bohr Institute—Nano-Science Center, University of Copenhagen, Universitetsparken 5, DK-2100 Copenhagen, Denmark

E-mail: lindelof@it.dk

Received 12 October 2007, in final form 29 November 2007
Published 1 April 2008
Online at stacks.iop.org/JPhysCM/20/164207

Abstract

Small deviations from the predictions of conductance quantization of three-dimensional saddle point potential theory measured in side-gated GaAlAs quantum point contacts are reported. Particular emphasis is put on the so-called 0.7 structure and regular conductance oscillations on the quantized plateau. A similar temperature dependence of the oscillations and the 0.7 structure is observed. These oscillations give rise to Fabry–Perot type diamond patterns in bias spectroscopy plots and to oscillations versus bias for fixed gate voltage at conductances $G \ll 2e^2/h$. We discuss electron localization due to mismatch to the two-dimensional electron gas as the cause of the Fabry–Perot resonances. The two possibilities of a charge maximum (spin 1/2) and minimum in the middle of the constriction are suggested as the root of the 0.7 structure.

(Some figures in this article are in colour only in the electronic version)

Quantum point contacts (QPCs) take many types, shapes, and materials. All share the common feature of conductance quantization. The most prominent example is a constriction formed in a two-dimensional electron (hole) gas (2DE(H)G) by split gates or side gates to a GaAlAs heterostructure (Wharam *et al* 1988, van Wees *et al* 1988, Danneau *et al* 2007). Conductance quantization has also been reported in 3D break junctions, cleaved edge overgrowth GaAlAs samples, and carbon nanotubes. The conductance quantization is never accurate as in the quantum Hall effect. This is because the quantization depends sensitively on the boundary condition between the 1D region and the source and drain contacts. Ideal conductance quantization is only possible, if the constriction cross section varies slowly over a Fermi wavelength from 1D to 3D (Glazman *et al* 1988). The only type of quantum point contact approaching this limit is the break junction, where, however, the dimensions and the Fermi wavelength are both typically on the atomic scale. A 3D constriction in a semiconductor has so far not been fabricated. The accuracy of conductance quantization will, even in the ideal cases, be limited by tunneling and thermal activation over the barrier in the 1D region. Because none of the quantum point contacts so far fabricated are ideal, it is perhaps not surprising that deviations from ideal conductance quantization are the rule rather than the exception (Fitzgerald 2002, Berggren and Pepper 2002).

A theoretical model from which all deviations may be counted is the so-called saddle point potential model, in which we describe the potential in the vicinity (within a few times the Fermi wavelength) of the constriction by a quadratic saddle point with curvatures ω_x and ω_y. Many 3D saddle point potentials have been used in the literature, and this model of penetration through a barrier (by thermal or tunneling processes) goes back to the theories of nuclear fission barriers (Hill and Wheeler 1953). In the single electron approximation, the transmission through the constriction (top point of the saddle potential) can be analytically calculated and yields the following simple expression (Büttiker 1989):

$$G = \sum_n \frac{2e^2}{h} \int_0^\infty (1 + \mathrm{e}^{-2\pi\varepsilon_n})^{-1} \left(-\frac{\partial f(E,T)}{\partial E}\right) \mathrm{d}E \quad (1)$$

where

$$\varepsilon_n = \frac{(E - \hbar\omega_y(n + \frac{1}{2}) - V_0)}{\hbar\omega_x}$$

and where $f(E,T)$ is the Fermi function, E is the energy determined by the gate voltage, T the temperature, V_0 is a constant potential and $n = 1, 2, 3 \ldots$.

Very few attempts have been made to fit this expression to the conductance versus gate voltage and temperature. This may be due to the various deviations mentioned below, which makes such a fit difficult. The main cause of deviations are impurity potentials, which strongly distort the saddle potential, giving rise to violent fluctuations in the conductance, and obscures the conductance quantization (Nixon *et al* 1991). Generally, these fluctuations, which are observed at low temperatures, are smeared by increasing the temperature. Thermal smearing is already included in equation (1), and has been studied in an attempts to fit the conductance versus gate voltage and determine ω_x and ω_y (Taboryski *et al* 1995). Another way of smearing the fluctuations in the conductance, when plotted versus gate voltage, is by adding a small magnetic field (∼0.1 T). When the magnetic flux through the constriction region approaches a flux quantum, the resonances are smoothed due to phase randomization, and the conductance quantization versus gate voltage becomes more horizontal.

Over the last few years GaAlAs quantum point contacts with very few or zero impurities near the constriction have been fabricated and studied. Such perfect samples are the prerequisite for studying intrinsic deviations from the saddle point potential model. A distinct deviation from the prediction of the saddle point potential model was studied by Thomas *et al* (1996), namely the so-called 0.7 structure, which we shall exemplify in the following. We further present a new Fabry–Perot type resonance observed in quantum point contacts, but not studied in detail earlier.

One should bear in mind that even without impurities and with a perfectly smooth saddle point potential (no edge irregularities), there is a QPC requirement that the variation of the potential leading up to the saddle point should be slow on the scale of the local Fermi wavelength. In the cases, where this has been studied for quantum point contacts, this is only marginally fulfilled. Because the electrodes are 2DEGs, the potential is not a quadratic saddle potential, and the adiabatic assumption of the QPC is valid only a few Fermi wavelengths from its center; this will lead to reflections. This, as we discuss later, may in turn lead to a weak confinement of charge in the constricted region. Another deviation related to the contacts between the point contact and the electrodes has been observed for cleaved edge 1D channels depleted by a top Mo gate (de Picciotto *et al* 2005). Here clear quantization of conductance is observed but at 10–30% too low a value. This also has to do with the boundary condition at the end of the 1D channel, where the electrons must be scattered out in the 2D plane of the quantum well in the cleaved heterostructure. The cleaved edge 1D constriction exhibits a 0.7 structure on top of the 10–30% reduced quantized conductance value.

Figures 1(A) and (B) show the conductance of a side-gated QPC seen in the SEM picture of the inset to figure 1(B). The QPC is formed in a modulation doped 2DEG with mobility, $\mu = 70\ \mathrm{m^2\,V^{-1}\,s^{-1}}$, and a carrier density of $n_2 = 1.9 \times 10^{15}\ \mathrm{m^{-2}}$. The 2DEG is separated by 75 nm from the (100)-surface of the heterostructure. By e-beam lithography and etching two V-shaped trenches separate the side gates from the constriction. The effective width and length of the constriction is ∼200 nm. By using such a V-shaped trench etched quantum point contact we minimize the

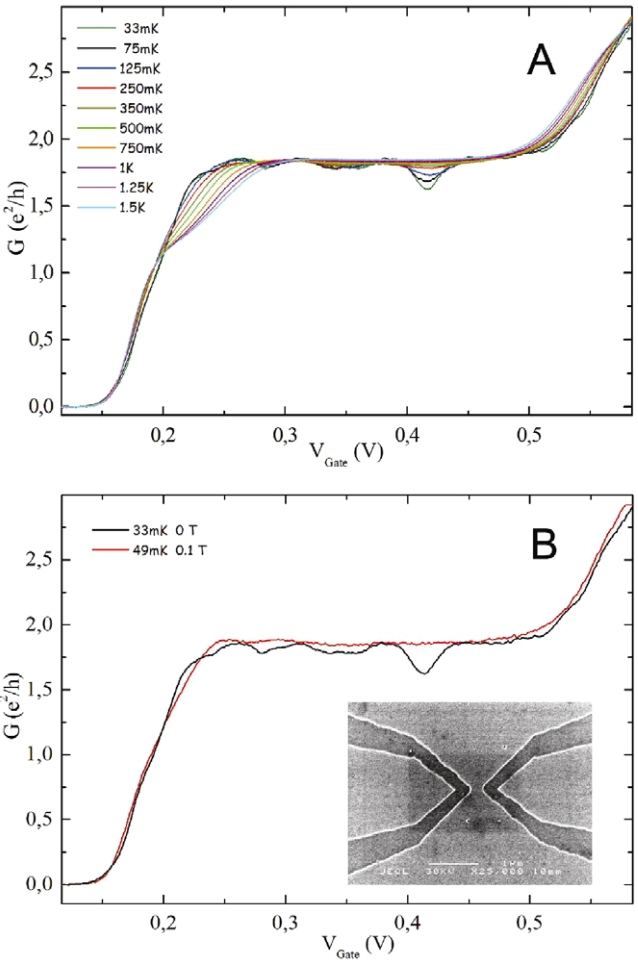

Figure 1. Experimental conductance traces of as a function of side gate voltages for a trench etched quantum point contact. A scanning electron microscope (SEM) picture of the quantum point contact is shown in the inset to figure 1(B). Outside the two dark V-shaped trenches in the SEM picture, there is a two-dimensional electron gas (2DEG) with a carrier density of $1.9 \times 10^{15}\ \mathrm{m^{-2}}$ and a mobility of $70\ \mathrm{V\,s\,m^{-2}}$. The grey square is from the exposure in taking the SEM picture. No series resistance has been subtracted from the data. (A) shows a series of conductance versus side gate voltage all exhibiting a clear conductance quantization at $2e^2/h$. The different traces are taken at temperatures between 0.033 and 1.5 K, and clearly exhibit an enhanced resonant structure on top of the conductance quantization as temperature is lowered. At the highest temperature (1.5 K) the transition from high transconductance ($\mathrm{d}G/\mathrm{d}V_{\mathrm{Gate}}$) to almost zero transconductance is smoothed by the 0.7 structure starting around $G = 0.7\ 2e^2/h$. The 0.7 structure goes away as temperature is lowered, almost simultaneously with the appearance of the resonances. (B) shows two traces of conductance versus side gate voltage with and without a magnetic field of 0.1 T perpendicular to the 2DEG. A magnetic field of only 0.1 T smooth out the resonances indicating that they have an extension of about 0.04 $\mu\mathrm{m}^2$ or 200 nm in linear extension. The distance between the minima in the resonances along the side gate voltage axis are 0.05 V corresponding to an energy of 0.1 meV, which for a Fabry–Perot resonance in the region of the 2DEG would correspond to reflectors 200 nm apart.

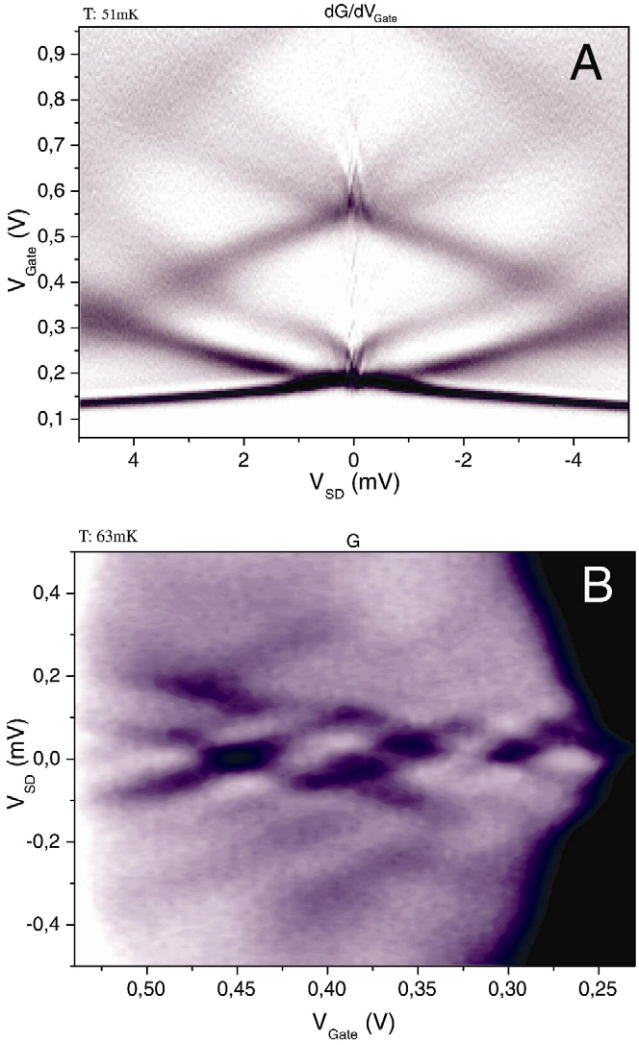

Figure 2. (A) Transconductance (dG/dV_{Gate}) in a grey-scale plot versus source–drain voltage, V_{SD}, and side gate voltage, V_{Gate}. Dark is large transconductance and white is zero transconductance. This is often called a bias spectroscopy plot. The large diamond-like white region is surrounded by dark lines, where the lowest energy of the first or second one-dimensional subband in the middle of the point contact equals the chemical potential of source or drain. The additional lines in the two diamonds, which looks like parabolas in the V_{SD}–V_{Gate} coordinate system are related to the 0.7 structure. A weak resonance feature is seen for small V_{SD} and almost everywhere along the V_{Gate} axis; this corresponds to the resonant structure displayed also in figures 1(A) and (B). (B) Enlarged region from (A) to show the resonant oscillations in the first diamond. Here the conductance is displayed in a grey-scale representation (black is minimum conductance) versus V_{Gate} and versus V_{SD} ((B) is turned 90° anticlockwise relative to (A)). The oscillations in this grey-scale plot exhibit small Fabry–Perot resonant tunneling diamonds. The energy periods of the resonance can be read off along the V_{SD} axis to be 0.1 meV.

chance that we have a charged impurity in the near vicinity of the two-dimensional constriction. The overall shape of the conductance versus the side gate voltage (both side gates connected) is typical of a well-behaved QPC. Figure 1(A) shows a series of G versus V_{Gate} characteristics at different temperatures. As first noted by Thomas *et al* (1996) a smooth transition from $G = 0$ to $2e^2/h$ at very low temperature changes at higher temperatures into a characteristic feature above $G = 0.7\,2e^2/h$. This 0.7 structure is also observed at the higher order conductance plateaus (Kristensen *et al* 1998a). The suppression from $2e^2/h$ to $0.7\ 2e^2/h$ has an activated behaviour, which depends on the gate voltage. This activation energy increases roughly as V_{Gate}^2, i.e. roughly quadratic in the density in the middle of the constriction (Kristensen *et al* 1998b). The G versus V_{Gate} at the lowest temperatures follow roughly the prediction of the parabolic saddle potential, but with a characteristic temperature, T^*, which is higher than the experimental value. Another deviation from the prediction of the saddle point potential model is the appearance of conductance fluctuations on top of the quantized conductance plateau. These fluctuations can be quite violent and often obscure the conductance quantization. For the most regular samples like the one in figure 1 the fluctuations take the form of a simple oscillation with an energy periodicity of typically 0.1 meV. It is generally believed that these fluctuations spring from the irregular side gate geometry or from electrostatic impurities. The regular oscillations seen in figure 1(A) are however always observed even in the most perfect QPC and indicate that this is an intrinsic behaviour created by the violation of the adiabatic assumption, i.e. that the change in the constriction width happens on a scale that is shorter or more abrupt than a few times the local Fermi wavelength. In fact, the perfect adiabatic assumption in the 3D saddle point model is never really fulfilled for constrictions in a 2DEG as mentioned above. A 3D point contact must have a cross section, which increases only little over a distance of the Fermi wavelength. Such samples have so far not been made.

The oscillations of G on top of the quantized conductance plateau are removed in a modest field of 0.1 T as seen in figure 1(B). This is a result of a weak localization type interference, where 0.1 T induces a flux quantum h/e in an area of the QPC. Since the width of the QPC is 200 nm, this leads to an effective total length of 200 nm. Such a length corresponds to the Fabry–Perot-like wavelength of the oscillation observed in figure 1(A) on top of the conductance plateau. We believe that the periodic variation of the oscillation is an intrinsic property of a perfect, smooth, and impurity-free QPC made in a 2DEG. The Fabry–Perot oscillations on the plateau conductance appear as sharp dips in the conductance at regular intervals, and the temperature dependence is anti-correlated with the appearance of the 0.7 structure as seen in figure 1(A). In fact, we can also roughly extract an activation energy (broadening) from the temperature dependence of the width of the oscillations, which is, however, smaller than the activation energy of the 0.7 structure. A magnetic field of 0.1 T does not affect the 0.7 structure. A magnetic field of 1–10 T creates a Zeeman splitting, which in turn creates a conductance plateau at $0.5\ 2e^2/h$. A smooth transition from 0.7 to 0.5 as the magnetic field is increased to 10 T, has often been taken as a proof of the 0.7 structure already signals a spin-polarized state at 0 T (Thomas *et al* 1996).

A regular conductance oscillation is observed on the quantized conductance plateau in perfect samples. It seems therefore to be an intrinsic property of a QPC and not created by impurities or an irregular side gate geometry. This is further supported by our bias spectroscopy investigations figures 2 and 3.

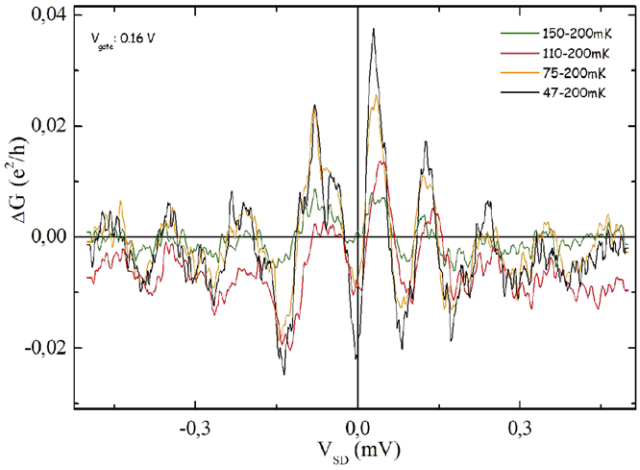

Figure 3. Change in conductance with temperature of a quantum point contact (QPC, see inset to figure 1(B)) plotted as a function of source–drain voltage, V_{SD}. The plotted change in conductance, ΔG, is a result of changing the temperature of the QPC between a low temperature (47, 75, 110 and 150 mK) and 200 mK and plotting the difference in conductance. The side gate voltage, V_{Gate}, is fixed at a value (0.16 V) which place the QPC at $G \sim 0.2\ e^2/h$. The observed oscillations of the conductance with V_{SD} have the same origin as the resonances seen in figure 2(B). However, the oscillations at these low gate voltages are not visible in figures 1(A), (B) and 2(A), (B), and can only be seen here thanks to our differential measuring technique. The activation energy of these resonances is similar to the energy of the Fabry–Perot pattern in figure 2(B) and smaller than the activation energy of the 0.7 structure.

Figure 2(A) shows the transconductance in a grey-scale representation as a function of the side gate voltage (y-axis) and source drain voltage (x-axis) (a bias spectroscopy plot) at $T = 47$ mK. The QPC is seen in a SEM photo in figure 1(B) (inset). The sharp changes in conductance in figure 2(A) is the darker region. The saddle point potential model explains the basic diamond structure (with a $G = 2e^2/h$ plateau). The top point of the diamond at $V_{SD} = \pm 4.5$ mV and $V_{Gate} = 0.35$ V, is where the 1D singularity in the density of state in the middle of the QPC of first and second 1D subband hit the Fermi energy in the source and the drain respectively. There is a top point in a smaller diamond at $V_{SD} = \pm 3$ mV and $V_{Gate} = 0.43$ V where the 1D singularity in the density of state of the second 1D subband in the middle of the QPC reaches another peak in the density of state related to the 0.7 feature. The same behaviour is seen repeated in the second diamond ($G = 4e^2/h$). A characteristic V-shaped curve of maximum $\mathrm{d}G/\mathrm{d}V_{Gate}$ is seen at the very start of the conductance plateau of the QPC at $V_{SD} = 0$ and $V_{Gate} = 0.2$ V as well as at $V_{SD} = 0$ and $V_{Gate} = 0.65$ V. This is directly the signature of the 0.7 structure (figure 1(A), 1.5 K), which is observed at higher temperatures and appears in this bias spectroscopy plot at higher temperatures as a simple smearing of this V-shaped feature. Whereas the 0.7 structure as a function of V_{Gate} at $V_{SD} \sim 0$ and measured at elevated temperatures is often strongly perturbed due the irregularities and impurities close to the QPC, its features in the bias spectroscopy plot are always there, at least for QPCs with the geometry similar to figure 1(B) (inset). Being thus more robust, it may be argued that these features in the bias spectroscopy plots are more fundamental for an understanding of the 0.7 structure than the G versus V_{Gate} anomalies.

Another more feeble feature, not predicted by the saddle point potential model, is seen in figure 2(A) in the region of small V_{SD} (± 0.5 mV) and in a wide range of gate voltages. The structure appears to reflect a Fabry–Perot mode with sharp dips in conductance as seen in figure 2(B) as already noted in figure 1(A). For the QPCs with the smallest random fluctuations such oscillations are always visible at the lowest temperatures. These structures grow to a detectable level around the same low temperature as where the 0.7 structure disappears (see figure 1(A)). We have also conducted experiments at fixed gate voltages. To enhance sensitivity we have made a differential measurement, where the conductance at $T = 200$ mK and at a number of lower temperatures have been subtracted from each other. Such a series of differential measurements are shown as a function of V_{SD} in figure 3. As seen, the conductance oscillations grow as temperature is lowered, and the oscillations are indeed very regular, and seen at a low conductance ($G \sim 0.2\ e^2/h$), where the oscillations are not directly visible as in figures 2(A) and (B). This consolidates our belief that for such very clean QPCs these oscillations are intrinsic to the QPC and determined by an effective length of the QPC. In order to calculate the resonance energies, the variation of the Fermi energy with distance from the center of the QPC must be taken into account. In addition, the geometrical shape of the QPC is important. An approximate characteristic length of 300 nm seems meaningful. Within a length of ± 300 nm, there are around two electron charges at $V_{Gate} = 0.16$ V. We believe the Coulomb blockade energy for these charges is smeared due to the large transmission to the source and drain 2DEG and therefore only directly visible in the region for very small conductance (Gloos *et al* 2006, Yoon *et al* 2007). Our very regular conductance oscillations in a QPC also focuses attention to the importance of the intrinsic potential landscape in the close vicinity of an ideal QPC made from a 2DEG.

The very regular Fabry–Perot data around the 0.7 structure of the QPC seen in all quantum point contacts at very low temperatures is puzzling and can hardly be related to random impurities in the vicinity of the quantum point contact. In stead it gives indication for a standing electron wave (eigenenergy) between two level branching points on each side of the QPC (here estimated to be 300 nm away) and give reason to believe that a weakly localized number of electrons are present in the QPC near pinch off. This may be described by the Wigner lattice approach by Matveev (2004). There is an additional boundary condition given by the symmetry of the QPC. The electronic eigenenergy wavefunction may have either a minimum or a maximum density in the center of the QPC, where there is a potential maximum. This gives always two solutions (isomers), which may be separated by some tenths of meV. This energy difference is smallest for the lowest density and increase as the electron density in the middle of the constriction increases and screening is strong. The state with a minimum in the electron density in the middle of the constriction will have the lowest energy. The two

configurational states are not there simultaneously, but there will be a thermal fluctuation between these two isomers as pointed out by Lindelof (2001). This picture does not need the spin polarization picture, which has been the dominating belief since the pioneering work of Thomas *et al* (1996) and the theoretical studies by Wang and Berggren (1998) and by Reimann *et al* (1998). The 0.7 structure may come from thermal occupancy of these two configurations of the QPC. There is a thermal fluctuation between the two isomers such that the conductance jumps between the values given by one or the other. The isomer with a localized electron (and a spin $\frac{1}{2}$) in the middle of the constriction is the thermally excited configuration, which will give rise to a Kondo type transmission (Cronenwett *et al* 2002), if at all populated. The ground state configuration gives a conductance quantization in the usual way at low temperatures.

Acknowledgments

We thank Kurt Gloos for valuable help with experiments. Discussions with Alex Hamilton are appreciated. The research was supported by the following EU grants: Ultra-1D, CARDEQ, SECOQC and a grant from the Danish Research Council (FTP).

References

Berggren K and Pepper M 2002 New directions with fewer dimensions *Phys. World* **15** (October) 37–42

Büttiker M 1989 Quantized transmission of a saddle-point constriction *Phys. Rev.* B **41** 7906–11

Cronenwett S M, Lynch H J, Goldhaber-Gordon D, Kouwenhoven L P, Marcus C M, Hirose K, Wingreen N S and Umansky V 2002 Low temperature fate of the 0.7 structure in a point contact: a Kondo-like correlated state in an open system *Phys. Rev. Lett.* **88** 226805

Danneau R, Klochan O, Clarke W R, Ho L O, Micolich A P, Simmons M Y, Hamilton A R, Pepper M and Ritchie D A 2007 Enhanced g-factor near the 0.7 structure in ballistic hole quantum wires *Preprint* cond-mat/0702210v2 pp 1–4

de Picciotto R, Pfeiffer L N, Baldwin K W and West K W 2005 Temperature-dependent 0.7 structure in the conductance of cleaved-edge-overgrowth one-dimensional wires *Phys. Rev.* B **72** 033319

Fitzgerald R 2002 Quantum point contact mysteries reexamined *Phys. Today* **55** (May) 21–3

Glazman L I, Lesovik G B, Khmelnitskii D E and Shekhter R I 1988 Reflectionless quantum transport and fundamental ballistic-resistance steps in microscopic constrictions *JETP Lett.* **48** 238–41

Gloos K, Utko P, Sørensen C B, Hansen J B and Lindelof P E 2006 Current–voltage characteristics of quantum-point contacts in the closed-channel regime: transforming the bias voltage into an energy scale *Phys. Rev.* B **73** 125326

Hill D L and Wheeler J A 1953 Nuclear constitution and the interpretation of fission phenomena *Phys. Rev.* **89** 1102–45

Kristensen A, Jensen J B, Zaffalon M, Sørensen C B, Reimann S M and Lindelof P E 1998a *J. Appl. Phys.* **83** 607–9

Kristensen A, Lindelof P E, Jensen J B, Zaffalon M, Hollingbery J, Pedersen S W, Nygård J, Bruus H, Reimann S M, Sørensen C B, Michel M and Forchel A 1998b *Physica* B **249** 180–4

Lindelof P E 2001 Effect on conductance of an isomer state in a quantum point contact *Proc. SPIE Int. Soc. Opt. Eng.* **4415** 77–85 (see www.lindelof.info)

Matveev K A 2004 Conductance of a quantum wire in the Wigner-crystal regime *Phys. Rev. Lett.* **92** 106801

Nixon J A, Davies J H and Baranger H U 1991 Interaction effects in a one-dimensional constriction *Phys. Rev.* B **43** 12638

Reimann S M, Koskinen M, Lindelof P E and Manninen M 1998 Spin-density waves in superdeformed quantum dots *Physica* E **2** 648–51

Taboryski R, Kristensen A, Soerensen C B and Lindelof P E 1995 Conductance-quantization broadening mechanisms in quantum point contacts *Phys. Rev.* B **51** 2282–6

Thomas K J, Nicholls J T, Martin-Moreno L, Pepper M, Frost J E F, Ritchie D A and Jones G A C 1996 Possible spin polarization in a one-dimensional electron gas *Phys. Rev. Lett.* **77** 135–8

van Wees B J, van Houten H, Beenakker C W J, Williamson J G, Kouwenhoven L P, van der Marel D and Foxon C T 1988 Quantized conductance of point contacts in a two-dimensional electron gas *Phys. Rev. Lett.* **60** 848–51

Wang C K and Berggren K F 1998 Local spin polarization in ballistic quantum point contacts *Phys. Rev.* B **57** 4552–5

Wharam D A, Thornton T J, Newbury R, Pepper M, Ahmed H, Frost J E F, Hasko D G, Peacock D C, Ritchie D A and Jones G A C 1988 One-dimensional transport and the quantization of the ballistic resistance *J. Phys. C: Solid State Phys.* **21** L209

Yoon Y, Mourokh L, Morimoto T, Aoki N, Ochiai Y, Reno J L and Bird J P 2007 Probing the microscopic structure of bound states in quantum point contacts *Phys. Rev. Lett.* **99** 136805